CYCLIC SPECTRAL ANALYSIS FROM THE AVERAGED CYCLIC PERIODOGRAM

Roger Boustany, **Jérôme Antoni**

University of Technology of Compiègne
60205 Compiègne, France

Abstract: The theory of cyclostationarity has emerged as a new approach to characterizing a certain type of nonstationary signals. Many aspects of the spectral analysis of cyclostationary signals have been investigated but were essentially based on the use of the smoothed cyclic periodogram. This paper proposes a cyclic spectral estimator based on the averaged cyclic periodogram which benefits from better implementation properties. It shows that an unexpected but important condition for this estimator to be valid is to set enough overlap between adjacent segments in order to prevent cyclic leakage. It proves that setting the percentage of overlap to 75% with a hanning window, or 50% with a half-sine window fixes the problem. It also shows that in certain situations the cyclic leakage associated with the averaged cyclic periodogram can be made exactly zero, in contrast with the smoothed cyclic periodogram. Illustrative examples finally confirm the obtained results, where it is also demonstrated how to use them for efficiently estimating the Wigner-Ville spectrum.

Keywords: Signal processing, Spectral analysis, Averaged periodogram, Cyclostationary signals, Cyclic spectral estimation, Cyclic leakage

1. INTRODUCTION

During the last two decades, the theory of cyclostationarity has emerged as a new approach to characterizing a certain type of nonstationary signals (Gardner, 1991),(Gardner, 1990),(Giannakis, 1998). Cyclostationarity extends the class of stationary signals to those signals whose statistical properties change periodically with time. Such signals are generally not periodic but random in their waveform, yet they are inherently generated by some periodic mechanism.

As opposed to stationary signals, CS signals contain extra information due to their hidden periodicities. In the time domain, this extra information is carried by the temporal variations of statistical descriptors such as the instantaneous auto-correlation function (Gardner, 1990). Very interestingly, the same information relates in the frequency domain to correlations between spectral components spaced apart by specific frequencies, referred to as *cyclic frequencies* (Gardner, 1991). As opposed to general nonstationary signals, CS signals also enjoy a well-understood theory which actually generalizes all the signal processing tools historically developed for stationary signals. In particular, the very powerful spectral analysis of stationary signals finds an interesting generalization. Actually many aspects of the spectral analysis of CS signals have already been investigated in the specialized literature (Gardner, 1986), (Hurd, 1989), (Roberts *et al.*, 1991), (Dandawate and Giannakis, 1994) but they were mainly based on the smoothed cyclic periodogram. The aim of this paper is to study the averaged cyclic periodogram as an estimator of the cyclic spectrum. The reason for this choice is that the averaged

periodogram is the most popular technique for the spectral analysis of stationary signals due to its high computational efficiency, its robustness against outlying data and its ability to remove non stationary trends. As far as we know, the averaged cyclic periodogram has been rarely advocated in the cyclostationary literature.

The paper is organized as follows. In section 2, the basic terminology of cyclostationary signals are reviewed. In section 3, an averaged cyclic periodogram is established on the basis of a general quadratic form for cyclic spectral estimation. In section 4, the spectral estimator introduced in section 3 is studied in terms of bias and variance. Finally, illustrative examples are provided in section 5.

2. CYCLOSTATIONARY SIGNALS AND THEIR TERMINOLOGY

In the following we will consider sampled signals with Δ denoting their sampling period and n their temporal index. For simplicity we shall only consider signals with zero mean and therefore restrict our analysis to purely random signals. This assumption is without loss of generality since efficient techniques exist for centering non-zero mean cyclostationary signals (Antoni *et al.*, 2004). Stricto sensu, a cyclostationary (CS) signal $X[n]$ is a signal whose joint probability density function is a quasi-periodic function of time. This entails that any typical statistical descriptor of signal $X[n]$ is also a quasi-periodic function of time in particular the instantaneous auto-correlation function

$$\mathcal{R}_{2X}[n,\tau] = \mathbb{E}\left\{X[n+\beta\tau]X[n-\overline{\beta}\tau]^*\right\} \quad (1)$$

(where $\beta + \overline{\beta} = 1$, the parameter β allowing for a general formulation of various equivalent definitions) accepts a Fourier series

$$\mathcal{R}_{2X}[n,\tau] = \sum_{\alpha_i \in \mathcal{A}} R_{2X}[\tau;\alpha_i] e^{j2\pi\alpha_i n\Delta} \quad (2)$$

over the spectrum $\mathcal{A} = \{\alpha_i\}$ of *cyclic frequencies* α_i associated with the non-zero Fourier coefficients $R_{2X}[\tau;\alpha_i]$ known as the *cyclic auto-correlation functions* or *cyclo-correlation functions* of signal X. The Fourier transform of the cyclic auto-correlation function is a spectral descriptor of signal X and is known as the *cyclic power spectrum* or *cyclo-spectrum*

$$S_{2X}(f;\alpha_i) = \Delta \sum_{\tau=-\infty}^{\infty} R_{2X}[\tau;\alpha_i] e^{-j2\pi f\tau\Delta} \quad (3)$$

The next section will focus on estimating the cyclic power spectrum using the averaged cyclic periodogram on the basis of a general quadratic form.

3. CYCLIC SPECTRAL ESTIMATION USING THE AVERAGED PERIODOGRAM

3.1 A General Quadratic Form

We claim that any non-parametric estimator $\hat{S}_{2X}(f;\alpha;L)$ of the cyclic spectrum $S_{2X}(f;\alpha)$ can be deduced given a finite-length signal $\{X[n]\}_{n=0}^{L-1}$ from the general quadratic form

$$\hat{S}_{2X}(f;\alpha;L) = \Delta \sum_{p=0}^{L-1}\sum_{q=0}^{L-1} Q_L[p,q]X[p]X[q]^* \; e^{-j2\pi(f+\overline{\beta}\alpha)p\Delta} e^{j2\pi(f-\beta\alpha)q\Delta} \quad (4)$$

where Q_L is a suitably chosen positive semi-definite kernel such as to preserve the interpretation of $\hat{S}_{2X}(f;\alpha;L)$ as a power density and in particular $\hat{S}_{2X}(f;0;L) \geq 0$ for $\alpha = 0$. Let us define also $\mathcal{Q}_L(\lambda,\eta)$ the double DTFT (Discrete Time Fourier Transform) of kernel Q_L which will be used hereafter:

$$\mathcal{Q}_L(\lambda,\eta) = \Delta^2 \sum_{p=0}^{L-1}\sum_{q=0}^{L-1} Q_L[p,q] e^{-j2\pi\lambda(p-q)\Delta} e^{-j2\pi\eta q\Delta} \quad (5)$$

Different kernels Q_L result in different spectral estimators. Due to space limitations, we only consider here the case of the averaged cyclic periodogram. A more complete study will be presented in another paper.

Let $\{w[n]\}_{n=0}^{N_w-1}$ be a positive and smooth N_w-long data-window and let $w_k[n] = w[n-kR]$ be its shifted version by R samples. Then the averaged cyclic periodogram is

$$\hat{S}_{2X}^{(W)}(f;\alpha;L) = \frac{1}{K\Delta}\sum_{k=1}^{K} X_{N_w}^{(k)}(f+\overline{\beta}\alpha) X_{N_w}^{(k)}(f-\beta\alpha)^* \quad (6)$$

with $X_{N_w}^{(k)}(f) = \Delta\sum_{n=R}^{R+N_w-1} w_k[n]x[n]e^{-j2\pi f n\Delta}$ the short-time DTFT of the k^{th} weighted sequence $\{w_k[n]x[n]\}_{n=R}^{R+N_w-1}$ and $K = \lfloor (L-N_w)/R \rfloor + 1$ (where $\lfloor y \rfloor$ stands for the greatest integer smaller than or equal to y). The averaged cyclic periodogram is obtained from (4) wherein

$$Q_L[p,q] = \frac{1}{K}\sum_{k=1}^{K} w_k[p]w_k[q] \Leftrightarrow \mathcal{Q}_L(\lambda,\eta) = W(\lambda)W(\lambda-\eta)^* D_K^{R\Delta}(\eta) e^{-j\pi\eta R\Delta(K-1)} \quad (7)$$

with $W(f)$ the DTFT of $w[n]$ and $D_K^{R\Delta}(\lambda) = K^{-1}\frac{\sin(\pi\lambda R\Delta L)}{\sin(\pi\lambda R\Delta)}$ the Dirichlet kernel. Formula (6) can be very efficiently implemented by means of the FFT algorithm by imposing N_w to be a power of 2. It remains to state which constraints must fulfil kernel Q_L such as to yield a valid spectral estimate in terms of (i) minimum estimation bias and (ii) minimum estimation variance.

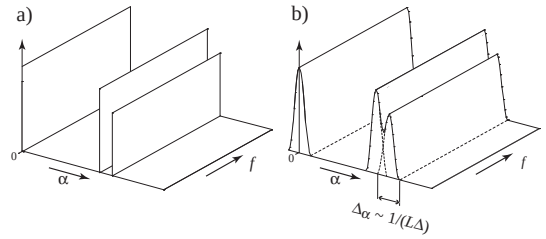

Fig. 1. Illustration of the effect of cyclic leakage.

3.2 Bias Analysis

For the proposed quadratic estimator to have minimum bias, it must hold that $\mathbb{E}\{\hat{S}_{2X}(f;\alpha;L)\} \simeq S_{2X}(f;\alpha)$ as closely as possible. Using Eqs.(4) and (5), it comes that:

$$\mathbb{E}\{\hat{S}_{2X}(f;\alpha;L)\} = \frac{1}{\Delta}\sum_{\alpha_i\in\mathcal{A}}\int_{\frac{-1}{2\Delta}}^{\frac{1}{2\Delta}} \mathcal{Q}_L(\lambda,\alpha-\alpha_i) \; S_{2X}(f-\lambda+\overline{\beta}(\alpha-\alpha_i);\alpha_i)d\lambda \quad (8)$$

This implies two conditions to be met, which we now investigate.

3.2.1. Condition I (power calibration) The first condition is to impose that the leading term indexed by $\alpha = \alpha_i$ equals $S_{2X}(f;\alpha)$. This yields $\sum_{p=0}^{L-1} Q_L[p,p] = 1$ which entails the well-known calibration $\|w\|^2 = \sum_n w[n]^2 = 1$.

3.2.2. Condition II (cyclic leakage minimization) The second condition is to impose that the terms indexed by $\alpha_i \neq \alpha$ in Eq.(8) be zero. Such terms may be interpreted as interferences resulting from the action of the smoothing kernel $\mathcal{Q}_L(\lambda,\eta)$ on the cyclic spectra positioned at cyclic frequencies $\alpha_i \neq \alpha$. The phenomena is akin to *energy leakage in the cyclic frequency*(see Fig.1); we shall refer to it *as cyclic leakage* as first discovered in reference (Gardner, 1986). It is in general impossible to make these interferences exactly zero (except in some special cases with the averaged cyclic periodogram as shown hereafter), however it is still possible to seek kernel Q_L such as to minimize them. To see this, let us consider the situation where $S_{2X}(f;\alpha) = S^{\alpha}_{2X}$ is a constant function in the f-frequency, so that condition II becomes that of making function

$$B_Q(\eta) = \frac{1}{\Delta}\int_{\frac{-1}{2\Delta}}^{\frac{1}{2\Delta}} \mathcal{Q}_L(\lambda,\eta)d\lambda \quad (9)$$

as close as possible to zero for any $\eta \neq 0$. This boils down to seeking kernel Q_L such as to minimize the bandwidth of $|B_Q(\eta)|$. In the case of the averaged cyclic periodogram:

$$|B_Q(\eta)| = \frac{1}{\Delta}\left|D_K^{R\Delta}(\eta)\right| \cdot |W_2(\eta)| \quad (10)$$

where $W_2(f)$ is the DTFT of $w[n]^2$. Although the Dirichlet kernel $D_K^{R\Delta}(\eta)$ has a narrow central lobe

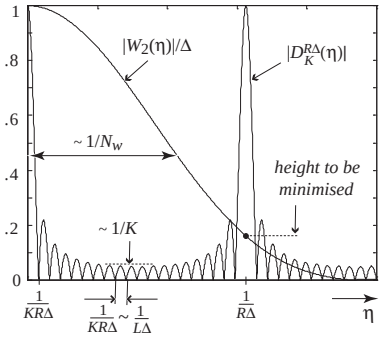

Fig. 2. Structure of function $B_Q(\eta)$ in the averaged cyclic periodogram.

of bandwidth $1/(KR\Delta) \sim 1/(L\Delta)$, it also has several other lobes with period $1/(R\Delta)$ - see Fig.2. It is therefore important that function $W_2(\eta)$ decreases fast enough in order to keep the effect of those secondary lobes as small as possible. Since the bandwidth of $W_2(\eta)$ is on the order of $1/N_w$, the condition is that $R \ll N_w$, i.e. important overlap must be placed on adjacent data-windows. In practice, $R = N_w/3$ (67% overlap) will be good enough with a Hanning or a Hamming data-window. With a half-sine data-window $R = N_w/2$ (50% overlap) will produce an excellent cyclic leakage minimization because the secondary lobes of $D_K^{R\Delta}(\eta)$ happen to fall on the nulls of $W_2(\eta)$. These results are illustrated in Fig.3 and summarized in the below table:

Secondary lobes roll-off for typical data-window

	Hamming	Hanning	half-sine
height of 2^{nd} lobe	-2.0 dB	-1.7 dB	-3.0 dB
height of 3^{rd} lobe	-8.8 dB	-7.8 dB	$-\infty$
height of 4^{th} lobe	$-\infty$	$-\infty$	$-\infty$

Therefore the following rule:

Proposition 1. For the averaged cyclic periodogram, Condition II requires that the acquisition time be long enough so that $L\Delta$ is significantly larger than the inverse of the minimum α-spacing - say $\Delta_\alpha^{\min}$ - to be resolved, that is $L\Delta \gg 1/\Delta_\alpha^{\min}$ and either $R \leq N_w/3$ with a Hanning and a Hamming data-window or $R \leq N_w/2$ with a half-sine data-window.

Last but not least, it is noteworthy that the averaged cyclic periodogram can be made *exactly unbiased* in α provided that the cyclic spectrum $\mathcal{A}$ is known. The idea is to choose $R\Delta$ such that $\Delta_\alpha^{\min}$ happens to coincide exactly with a zero of $D_K^{R\Delta}(\eta)$. For instance, one case of practical importance is when the signal of interest is periodically-correlated with a known cycle N, such that we have $\Delta_\alpha^{\min} = 1/(N\Delta)$. Then the following rule applies:

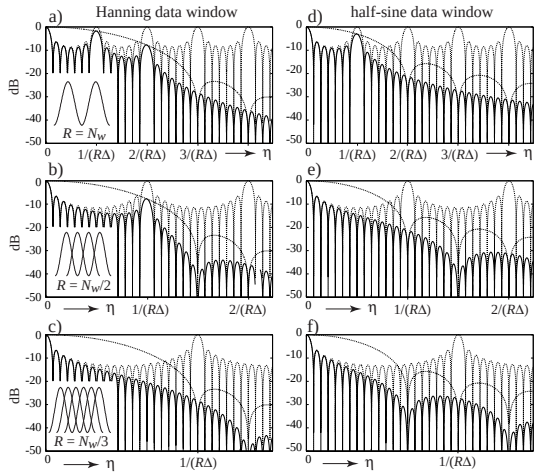

Fig. 3. Illustration of the effect of segments overlapping on cyclic leakage in the averaged cyclic periodogram: full lines = function $|B_Q(\eta)|$; dotted lines = functions $|D_K^{R\Delta}(\eta)|/\Delta$ and $|W_2(\eta)|$. Hanning window: a) no overlap, b) 50% overlap, c) 67% overlap. Half-sine window: d) no overlap, e) 50% overlap, f) 67% overlap.

Proposition 2. For a periodically-correlated signal with cycle N, setting $R = kN/K$, ($k \in \mathbb{N}$ but not a multiple of N) completely cancels the effect of cyclic leakage.

3.2.3. General bias evaluation Conditions I and II together guaranty that the proposed quadratic spectral estimator of the cyclic spectrum is unbiased in the case of CS *white* signals. The same conclusion obviously does not hold true in the general case of non-white signals.

Proposition 3. Provided that conditions I and II are met, the proposed quadratic spectral estimator has bias:

$$\mathbb{E}\{\hat{S}_{2X}(f;\alpha;L)\} - S_{2X}(f;\alpha) \simeq \frac{I_Q}{2}\frac{\partial^2}{\partial f^2}S_{2X}(f;\alpha) + \mathcal{O}(1/L)$$

with $I_Q = \Delta^{-1}\int_{-1/2\Delta}^{1/2\Delta}\lambda^2\mathcal{Q}_L(\lambda,0)d\lambda$ *the inertia of kernel* $\mathcal{Q}_L(\lambda,0)$.

The proof follows from a trivial Taylor expansion of Eq.(8). Proposition 3 generalises the bias formula known in the spectral analysis of stationary signals. However, care should be taken to meet condition II which protects against the effect of cyclic leakage, otherwise Eq.(3) becomes much more intricate. To our knowledge this point has rarely been addressed before.
Finally, provided that conditions I *and* II are met, the resolution in the α-frequency essentially depends on the acquisition time $L\Delta$, i.e. $\Delta_\alpha \sim 1/(L\Delta)$.

3.3 Variance Analysis

It finally remains to prove that the proposed quadratic estimator is consistent. We start with the following general result (the proof is not given here due to limited space):

Proposition 4. For large L:

$$Var\{\hat{S}_{2X}(f;\alpha;L)\}\simeq \mathcal{E}_{Q1}\cdot S_{2X}(f+\overline{\beta}\alpha;0)S_{2X}(f-\beta\alpha;0) + \mathcal{E}_{Q2}\cdot S_{XX^*}(f;\alpha)S_{XX^*}(f;\alpha)^*$$

where $\mathcal{E}_{Q1} = \frac{1}{\Delta^2}\iint_{-1/2\Delta}^{1/2\Delta}|\mathcal{Q}_L(\lambda,\eta)|^2\,d\lambda d\eta$ and $\mathcal{E}_{Q2} = \frac{1}{\Delta^2}\iint_{-1/2\Delta}^{1/2\Delta}\mathcal{Q}_L(\lambda,\eta)\mathcal{Q}_L(\lambda-\eta,-\eta)^* d\lambda d\eta$

The above formula reveals the existence of two terms carried by $\mathcal{E}_{Q1}$ and $\mathcal{E}_{Q2}$, respectively. However it happens that in many instances the second term is non-zero only on a countable set of frequencies in particular when the processes of interest are real. Hence the following result:

Proposition 5. For large L, the variance of $\hat{S}_{2X}(f;\alpha;L)$ is

$$Var\{\hat{S}_{2X}(f;\alpha;L)\}\simeq \mathcal{E}_{Q1}\cdot S_{2X}(f+\overline{\beta}\alpha;0)S_{2X}(f-\beta\alpha;0)$$

almost everywhere.

This very simple formula can be checked to generalize the result obtained for stationary signals ($\alpha = 0$) and also accepts the results of references (Hurd, 1989) and (Dandawate and Giannakis, 1994) as particular cases. It states that the variance of $\hat{S}_{2X}(f;\alpha;L)$ is proportional to the cross-spectra $S_{2X}(f+\overline{\beta}\alpha;0)$ and $S_{2X}(f-\beta\alpha;0)$ at frequencies $f+\overline{\beta}\alpha$ and $f-\beta\alpha$, and to the energy $\mathcal{E}_{Q1} = \|Q_L\|^2$ of kernel Q_L.
The particular expression taken by $\mathcal{E}_{Q1}$ in the case of the averaged cyclic periodogram becomes after some manipulations:

$$\mathcal{E}_{Q1} = \sum_{k=-K+1}^{K-1} R_w[kR]^2\cdot\frac{K-|k|}{K^2} \qquad (11)$$

where $R_w[k] = \sum_n w[n-k]w[n]$ is the autocorrelation function of the data-window $w[n]$. This result is valid for any value of R. Assessment of formula (11) with classical data-windows (e.g. Hanning, Hamming, half-sine) shows that $\mathcal{E}_{Q1}$ is a decreasing function of R/N_w where the minimum is virtually reached as soon as $R \le N_w/3$. For large L we have found that the minimum of $\mathcal{E}_{Q1}$ tends rapidly to $\|R_w\|^2/L$.

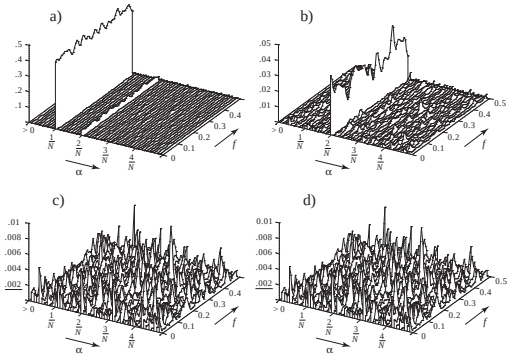

Fig. 4. Illustration of the effect of cyclic leakage on the estimated cyclic coherence function. The cyclic coherence function is that of a stationary signal and is theoretically zero everywhere ($\alpha \neq 0$). A Hanning data-window is used with a) $R = N_w$, b) $R = N_w/2$, c) $R = N_w/3$, and d) $R = N_w/4$.

4. ILLUSTRATIVE EXPERIMENTS

The first experiment has for objective to illustrate the necessity of properly setting the percentage of overlaps in the averaged cyclic periodogram. A stationary signal was synthesized ($\Delta = 1s$) and its cyclic coherence function ($\beta = 1/2$) - theoretically nil at $\alpha \neq 0$ - was computed for several values of alpha in the range $[0.001; 0.08]$ Hz in order to check for the presence of cyclostationarity:

$$\widehat{\gamma}_{2X}(f;\alpha;L) = \frac{\widehat{S}_{2X}(f;\alpha;L)}{\left[\widehat{S}_{2X}(f+\overline{\beta}\alpha;0;L)\widehat{S}_{2X}(f-\beta\alpha;0;L)\right]^{1/2}}$$

We used the averaged cyclic periodogram with the following settings: $N_w = 60$, a Hanning data-window, and FFT sizes of 128 samples; this provided a 1% level of significance of 0.002 to the cyclic coherence function. Different values of the increment parameter R were tested, i.e. $R = N_w$, $R = N_w/2$, $R = N_w/3$, and $R = N_w/4$. Results are displayed in Fig.4 for the four tested cases. As expected from the analysis of section 3.2, the case $R = N_w$ - Fig.4.a - produces significant cyclic leakage: instead of being statistically zero as expected from the theory, $\hat{\gamma}_{2X}(f;\alpha)$ carries a significant amount of "energy" at $\alpha = 1/N_w$ leaking from $\alpha = 0$. Similarly, a small amount of leakage - but still statistically significant (!) - is present at $\alpha = 2/N_w$. The same phenomena occurs at $\alpha = 2/N_w$ when $R = N_w/2$ - Fig.4.b. However as soon as $R \geq N_w/3$, it is checked that cyclic leakage virtually disappears as established in section 3.2 - Fig.4.c-d. Although not shown here very similar observations were obtained with a half-sine data-window except that cyclic leakage then disappeared for $R \geq N_w/2$ in accordance with the discussion of section 3.2. This experiment insists once again on the importance of correctly setting R in the averaged cyclic periodogram, a requirement that is truly specific to cyclic spectral analysis.

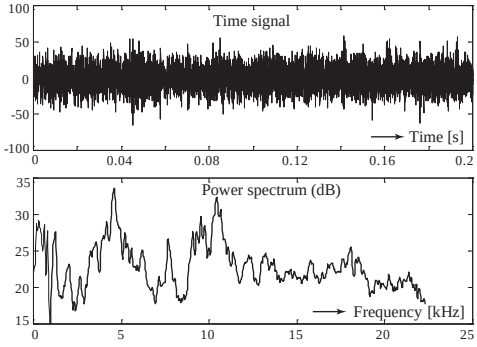

Fig. 5. a) Time signal and b) corresponding power spectrum computed from the averaged periodogram with a half-sine window of 1024 samples and 67% overlap. The frequency resolution is $\Delta_f \sim 0.1$ kHz. The 6-σ Confidence interval is $\simeq 2.6$ dB.

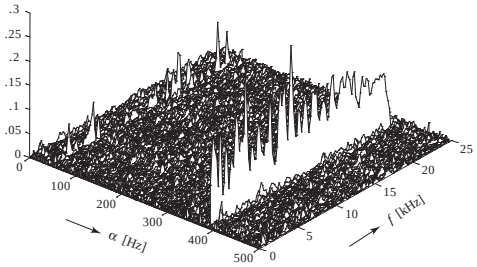

Fig. 6. Cyclic coherence function, computed from the averaged cyclic periodogram with a half-sine window of 256 samples and 67% overlap. The frequency resolution is $\Delta_f \sim 0.3$ kHz. The cyclic frequency resolution is $\Delta_\alpha \sim 1$ Hz. The 1% level of significance is 0.017.

The second experiment illustrates the use of cyclic spectral analysis on an industrial system. The system of interest is a hydraulic pump rotating at $\Omega \simeq 3000$ rpm to be monitored by means of vibration analysis. The vibration signal is captured by an accelerometer mounted on the pump casing and is sampled at a rate of 50 kHz. The first objective is to assess the origin of the pump vibrations, and secondly to characterize the "mechanical signature" of these vibrations. Figures 5.a and 5.b display 0.2 seconds of the vibration signal and the corresponding power spectrum, respectively. Inspection of these plots suggests that the signal essentially has a random structure: no clear harmonic structure is revealed in the spectrum, but two wide resonance peaks are found around 4.5 kHz and 10.5 kHz, the origin of which is to be investigated. To this purpose, the cyclic coherence function $\gamma_{2X}(f;\alpha)$ ($\beta = 1/2$) is computed for different values of α ranging from 1 Hz to 500 Hz with cyclic resolution $\Delta_\alpha = 1$ Hz. The result is displayed in Fig.6. There is clearly a region with high cyclic coherence at $\alpha = 391$ Hz, i.e. at eight

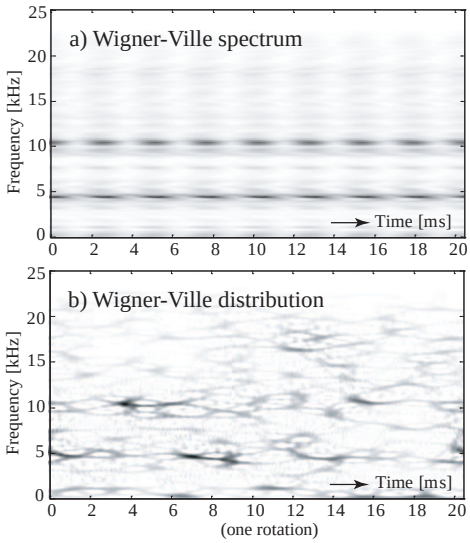

Fig. 7. a) Wigner-Ville spectrum from the analytic signal, synchronized on the blade passing frequency and displayed over one rotation. The frequency resolution is $\Delta_f \sim 0.3$ kHz. The finest time resolution is ~ 1 ms. Only values above 3 standard deviations of the stationary hypothesis are displayed. b) Smoothed pseudo-Wigner-Ville distribution displayed over one rotation. Frequency resolution $\Delta_f \sim 0.4$ kHz. The finest time resolution ~ 1 ms.

times the pump rotation speed. Note that this harmonic is not present in the power spectrum, so it does not relate to periodic vibrations but to some kind of periodic modulation of random carriers. The origin of this modulation is actually recognized as the passing frequency of the eight blades of the pump propeller, i.e. $8 \times \Omega = 391$ Hz, with $\Omega = 48.9$ Hz. Because the cyclic coherence function at $\alpha = 391$ Hz is above the 1% level of significance, it confirms that the vibration signal effectively exhibits a certain amount of cyclostationarity at this cyclic frequency. The final step is to characterize more finely the structure of this cyclostationary source by means of the Wigner-Ville spectrum

$$\begin{aligned}\mathcal{W}_{2X}[n,f) &= \mathcal{F}\{\mathcal{R}_{2X}[n,\tau]\} \\ &= \sum_{\alpha_i \in \mathcal{A}} \mathcal{F}\{R_{2X}[\tau;\alpha_i]\} = \sum_{\alpha_i \in \mathcal{A}} S_{2X}(f;\alpha_i).\end{aligned}$$

where $\mathcal{F}\{\cdot\}$ stands for the Fourier transform. The Wigner-Ville spectrum is computed by using α_i's equal to all multiples of 391 Hz so that the blade time-frequency signature can be extracted from the remaining signal. The result is displayed in Fig.7.a, revealing that the two resonance peaks initially detected in the power spectrum are linked to the blade activity; more specifically they are two random carriers which are periodically amplitude modulated with the blade passing frequency. Incidentally, Fig.7.b displays the smoothed pseudo-Wigner-Ville distribution computed on one rotation of the pump with similar time-frequency resolution in order to stress the fact that the proposed estimator of the Wigner-Ville spectrum drastically helps to suppress interference terms and consequently to improve the quality of the time-frequency lecture.

5. CONCLUSION

The purpose of this paper was to provide a cyclic spectral estimator based on the averaged cyclic periodogram - surprisingly rarely suggested in previous works. The conditions for this kernel to yield minimum bias and consistent estimators have been addressed in details. It was shown that by setting 50% overlap with a half-sine data window, or 67% overlap with a Hanning or a Hamming data-window, the averaged cyclic periodogram offers excellent cyclic leakage rejection; at the same time this precaution guarantees a nearly minimum estimation variance. Moreover, by providing the relevant conditions in designing kernel Q_L, the material presented herein leaves open a wide scope of possibilities for designing new and original cyclic spectral estimators.

REFERENCES

Antoni, J., F. Bonnardot, A. Raad and M. El Badaoui (2004). Cyclostationary modelling of rotating machine vibration signals. *Mechanical Systems and Signal Processing* **18**(6), 1285–1314.

Dandawate, A. and G. Giannakis (1994). Nonparametric polyspectral estimators for kth-order (almost) cyclostationary processes. *IEEE Trans. on Information theory* **40**(1), 67–54.

Gardner, W. (1986). Measurement of spectral correlation. *IEEE trans. on Acoustics, Speech, and Signal Processing* **34**(5), 1111–1123.

Gardner, W. (1990). *Introduction to Random Processes*. 2nd ed.. McGraw-Hill. Chap.12.

Gardner, W. (1991). Exploitation of spectral redundancy in cyclostationary signals. *IEEE Signal Processing Magazine* pp. 14–36.

Giannakis, G. (1998). Cyclostationary signal analysis. in *The Digital Signal Processing Handbook*, IEEE Press. Chap. 5.

Hurd, H. (1989). Nonparametric time series analysis for periodically correlated processes. *IEEE trans. on Information theory* **35**(2), 350–359.

Roberts, R., W. Brown and H. Loomis (1991). Computationally efficient algorithms for cyclic spectral analysis. *IEEE Signal Processing Magazine* pp. 38–49.